Cancer Letters ■■ (2015) ■■–■■

Contents lists available at ScienceDirect

Cancer Letters

journal homepage: www.elsevier.com/locate/canlet

Original Articles

Bone marrow derived myeloid cells orchestrate antiangiogenic resistance in glioblastoma through coordinated molecular networks

B.R. Achyut [a], Adarsh Shankar [a], A.S.M. Iskander [a], Roxan Ara [a], Kartik Angara [a], Peng Zeng [a], Robert A. Knight [b], Alfonso G. Scicli [c], Ali S. Arbab [a,*]

[a] Tumor Angiogenesis Laboratory, Biochemistry and Molecular Biology, Cancer Center, Georgia Regents University, Augusta, GA, USA
[b] NMR Center, Henry Ford Health System, Detroit, MI, USA
[c] Cellular and Molecular Imaging Laboratory, Henry Ford Health System, Detroit, MI, USA

ARTICLE INFO

Article history:
Received 24 June 2015
Received in revised form 29 August 2015
Accepted 9 September 2015

Keywords:
Glioblastoma
Resistance
Tumor angiogenesis
Bone marrow
VEGF
Tumor microenvironment

ABSTRACT

Glioblastoma (GBM) is a hypervascular and malignant form of brain tumors. Anti-angiogenic therapies (AAT) were used as an adjuvant against VEGF–VEGFR pathway to normalize blood vessels in clinical and preclinical studies, which resulted into marked hypoxia and recruited bone marrow derived cells (BMDCs) to the tumor microenvironment (TME). *In vivo* animal models to track BMDCs and investigate molecular mechanisms in AAT resistance are rare. We exploited recently established chimeric mouse to develop orthotopic U251 tumor, which uses as low as 5×10^6 GFP+ BM cells in athymic nude mice and engrafted >70% GFP+ cells within 14 days. Our unpublished data and published studies have indicated the involvement of immunosuppressive myeloid cells in therapeutic resistance in glioma. Similarly, in the present study, vatalanib significantly increased CD68+ myeloid cells, and CD133+, CD34+ and Tie2+ endothelial cell signatures. Therefore, we tested inhibition of CSF1R+ myeloid cells using GW2580 that reduced tumor growth by decreasing myeloid (Gr1+ CD11b+ and F4/80+) and angiogenic (CD202b+ and VEGFR2+) cell signatures in TME. CSF1R blockade significantly decreased inflammatory, proangiogenic and immunosuppressive molecular signatures compared to vehicle, vatalanib or combination. TCK1 or CXCL7, a potent chemoattractant and activator of neutrophils, was observed as most significantly decreased cytokine in CSF1R blockade. ERK MAPK pathway was involved in cytokine network regulation. In conclusion, present study confirmed the contribution of myeloid cells in GBM development and therapeutic resistance using chimeric mouse model. We identified novel molecular networks including CXCL7 chemokine as a promising target for future studies. Nonetheless, survival studies are required to assess the beneficial effect of CSF1R blockade.

Introduction

Glioblastoma (GBM), a grade IV glioma classified by World Health Organization (WHO), is considered highly malignant, vascular and invasive subtype [1]. GBM is most lethal during first year after initial diagnosis despite surgical resection, radiotherapy and/or chemotherapy [1,2]. Median survival of patients diagnosed with GBM is only 12–15 months [1,2]. Hypoxia and neovascularization are histopathologic features of GBM [3]. Anti-angiogenic therapies (AAT) were used as adjuvants mainly against VEGF–VEGFR pathway to normalize tumor vasculatures. However, all of them provided minimal to none effect with no change in overall survival [4,5]. Therefore, current challenge is to investigate mechanisms of undesirable outcomes in GBM clinical trials. Preclinical studies involving AATs have shown marked hypoxia, increased homing of bone marrow derived cells (BMDCs) to the tumor and activation of alternative pathways of neovascularization [6,7].

BMDCs play a pivotal role in tumor development [8] and endothelial progenitor cells (EPCs) from BM pool are recruited to tumor microenvironment (TME) [9–12]. BMDCs associated therapeutic resistance falls under evasive or adaptive resistance, where tumor itself after an initial response phase acquires evasive properties against therapeutic blockade by inducing alternate mechanisms that enable neovascularization, leading to renewed tumor growth and progression [13]. Distinct potential mechanism of resistance might be at cellular level [14] mediated through up-regulation of HIF1-α followed by induction of SDF1α, secretion of pro-angiogenic factors and recruitment of CXCR4+ BMDCs to the tumor [9–11,15]. These recruited cells were characterized as pro-angiogenic CD45+VEGFR2+ EPCs, or CD45+Tie2+ monocytes [16,17]. Interestingly, lin-ckit+Sca-1+ and their derived cells demonstrated recruitment to tumor but do not functionally contribute to tumor neovascularization [18]. BMDCs derived MMP9 modulates neovessel remodeling, thereby playing role in tumor growth [15,19].

* Corresponding author. Tel.: +1 706 721 8909; fax: +1 706 434 6406.
E-mail address: aarbab@gru.edu (A.S. Arbab).

http://dx.doi.org/10.1016/j.canlet.2015.09.004
0304-3835/

Studies have indicated that resistance to AAT has profound involvement of immune system [20–26]. Role of myeloid cells in tumor angiogenesis is an established phenomenon as shown by other authors [27–31] and supported by our previous study (unpublished), which showed that majority of bone marrow derived GFP+ cells acquire both myeloid signature (CD68) and endothelial signatures (CD202b and CD34) in the TME under vatalanib (VEGFR tyrosine kinase inhibitor) treatment. Tissue-resident macrophages originate from yolk-sac-derived erythro-myeloid progenitors [32], whereas, SDF-1 played an important role in the invasiveness of brain tumor and infiltration of macrophages from bone marrow [33]. AATs in glioma were associated with increased myeloid cell infiltration and stem cell accumulation [34]. However, investigations whether those phenotypes have bone marrow component, were lacking. In other study, authors noticed infiltration in myeloid populations in the tumor bulk and in the infiltrative regions after AAT [23]. Together, studies suggest that immune suppressive myeloid cells, especially myeloid derived suppressor cells (MDSCs) and tumor associated macrophages (TAM) [35–37], may participate in escape from AATs and represent a potential biomarker of resistance with potential therapeutic target in GBM [23,38].

Several chemokines such as macrophage colony-stimulating factor-1 (MCSF/CSF1) and monocyte chemotactic protein-1 (MCP1/CCL2) are known to contribute in the recruitment of TAMs to the tumor [39,40]. CSF1R expression has been reported on immunosuppressive myeloid cells and dendritic cells [41–43]. CSF1-CSF1R signaling regulates survival, differentiation, and proliferation of monocytes and macrophages [44,45], and have critical role in angiogenesis and tumor progression [46,47]. Therefore, the goals of the present study are to (1) investigate the effect of CSF1R blockade on orthotopic glioma development in a recently established preclinical chimeric mouse model, (2) to evaluate whether CSF1R blockade alone or in combination with VEGFR2 blockade could inhibit the homing of myeloid BMDCs to the glioma, (3) to identify signature immune cell populations following CSF1R inhibition that could have profound role in glioma growth and (4) to investigate key secreted molecular signatures in GBM TME following CSF1R inhibition.

Materials and methods

All animal related experimental procedures were approved by the Institutional Animal Care and Use Committee and Institutional Review Board of Georgia Regents University (animal protocol #2014-0625). All efforts were made to ameliorate suffering of animals. CO2 with secondary method was used to euthanize animals for tissue collection at the end of the study.

Establishing chimeric mouse

Chimeric mouse for orthotopic U251 glioma was established with IACUC approved protocol and published method [48]. Transgenic mice with universally expressing GFP under the human ubiquitin C promoter (C57BL/6-tg(UBC-GFP)30Scha) were used as donors (Jackson Laboratory, Maine, USA). Athymic nude mice (NCr-nu/nu) were used as recipients (Charles River, Frederick, MD, USA), and were whole body irradiated with sub-lethal dose of 6Gy (using Cs-137 source). After 24 hours, recipient mice were injected intravenous (n = 3) and intraperitoneal (n = 3) routes with BM cells (5×10^6 cells) collected from donor transgenic mice. All mononuclear cells were separated from red blood cells using lymphocyte cell separation media (Corning, Cellgro, USA), counted and 5×10^6 cells/100 µl were injected into each mouse. Ten microliter of blood (from orbital sinus) were collected from each mouse on days 7 to 56 (n = 3 each time point) following transplantation of BM to determine BM engraftment efficiency (GFP positivity) in peripheral blood using flow cytometer. Cells from athymic mice without irradiation and GFP+ cell transplantation were used as control for flow cytometry.

Animal model of human glioma

Precisely, animals were anesthetized with 100 mg/kg ketamine and 15 mg/kg xylazine i.p. The surgical zone was swabbed with betadine solution, the eyes coated with Lacri-lube and the animals were immobilized in a small animal stereotactic device (Kopf, Cayunga, CA). After draping, a 1-cm incision was made 2 mm to the right of the midline 1 mm retro-orbitally; the skull exposed with cotton-tip applicators and a 23G needle tip was used to drill a hole 2 mm to the right of the bregma, taking care not to penetrate the dura. A 10 µl Hamilton syringe with a 26G-needle containing tumor cells (2.4×10^5) in 3 µl was lowered to a depth of 2.5 mm, and then raised to a depth of 2 mm. During and after the injection, careful note was made of any reflux from the injection site. After completing the injection, we waited 2–3 minutes before withdrawing in a stepwise manner. The surgical hole was sealed with bone wax. Finally, the skull was swabbed with betadine before suturing the skin over the injection site.

In vivo *multispectral optical imaging*

Multispectral optical images were acquired using excitation profiles of 460–480 nm range and emission of 535 nm to monitor the GFP positivity on days 7, 14 and 21 after tumor cell implantation. RFP positivity was determined at excitation 587 nm and emission 610 nm. All optical imaging data were acquired by Spectral AMI (Spectral Instruments Imaging, LLC) machines and analyzed by AMI view software.

Drug treatments

Orthotopically implanted chimeric mice with U251 tumor cells were allowed to grow for 7 days and then started oral treatments of either vehicle or receptor tyrosine kinase inhibitors (vatalanib (50 mg/kg/day) [49], GW2580 (160 mg/kg/day) [43] and combination of both GW2580+ vatalanib, daily for two weeks. Seven days waiting period was followed after tumor implantation to mimic clinical scenario, where treatment is being done following detection of tumor.

In vivo *magnetic resonance imaging (MRI)*

All MRI experiments were conducted using a 7 Tesla 12 cm (clear bore) magnet interfaced to a varian console with actively shielded gradients of 49 gauss/cm and 100 µs rise times or a horizontal 7 Tesla BioSpec MRI spectrometer (Brucker Instruments, Billerica, MA) equipped with a 12 cm self-shielded gradient set (45 gauss/cm max). Detailed MRI procedure was adopted from our several previous publications [50–54]. An appropriate state of anesthesia was obtained with isoflurane (2.5% for induction, 0.7% to 1.5% for maintenance in a 2:1 mixture of N_2:O_2). After positioning using a triplanar FLASH sequence, MR studies were performed using pre-contrast T1, T2-weighted and post contrast T1-weighted MRI scans with following parameters (1) Standard T1-weighted multislice sequence (TR/TE = 500/10 ms, 256 × 256 matrix, 13–15 slices, 1 mm thick slice, 32 mm field of view (FOV), # of averages = 4). (2) T2-mapping sequence (2D multi-slice, multi-echo (MSME) sequence, TE = 10, 20, 30, 40, 50, 60 ms, TR = 3000 ms, 256 × 256 matrix, 13–15 slices, 1 mm thick slice, 32 mm field of view (FOV), # of averages = 2). Post contrast T1WI was used to determine volume of tumors in vehicle and drug treated mice by drawing irregular ROI to encircle whole tumor in each image section containing tumor using ImageJ software, and area was then multiplied by thickness of image slice to determine volume (cm^3). Two investigators blinded to the animal groups determined tumor volume.

Collection of GFP+ cells and determination of immune cell populations

Freshly isolated brain samples were separated into left and right (tumor bearing) hemispheres from each group and were homogenized to pass through 40 µm cell strainer to make single cell. Similarly, cells were collected from spleen and BM. Cells were labeled with antibodies (BioLegend) such as CD45, CD4, CD8, Gr1, CD11b, F4/80, CD68, CD133, CD31, CD34, CD202b (Tie2), and CD309 (VEGFR2) (other than FITC) to identify BM recruited cell types (GFP+) in the tumor as well as phenotypes of GFP+ cells in spleen and bone marrow. Flow cytometry data were acquired using Accuri C6 machine (BD Biosciences) and analyzed by BD Accuri C6 software.

Immunofluorescence study

After MRI at day 22, animals were euthanized and brains were collected for frozen tissue sections and later stained for immunofluorescence study to determine expression of myeloid cell signature markers CD11b (Abcam), F4/80 (Santa Cruz Biotechnology), p-ERK (Cell Signaling), Ki67 (DAKO), CXCL7 (Millipore) and CD31 (Abcam) at the site of tumor. Migration and incorporation pattern of GFP+ BMDCs was determined in different regions of the tumor.

Western blot analysis

Tumors were collected and processed for protein isolation using T-PER, tissue protein extraction reagent for tissue and Pierce RIPA buffer for tumor cells (Thermo Scientific, USA). Protein concentrations were estimated with Pierce, BCA protein assay kit (Thermo Scientific, USA) and separated by standard Tris/Glysine/SDS gel electrophoresis. Membranes were incubated with primary antibodies against IDO (1:1000, Santa Cruz Biotechnology), p-ERK and ERK (1:1000, Cell Signaling), and α-Tubulin (1:5000, Abcam) followed by horseradish peroxidase-conjugated secondary antibody (1:5000, Biorad). The blots were developed using a Pierce SuperSignal West Pico Chemiluminescent substrate kit (Thermo Scientific, USA). Western blot images were acquired by Las-3000 imaging machine (Fuji Film, Japan).

Please cite this article in press as: B.R. Achyut, Adarsh Shankar, A.S.M. Iskander, Roxan Ara, Kartik Angara, Peng Zeng, Robert A. Knight, Alfonso G. Scicli, Ali S. Arbab, Bone marrow derived myeloid cells orchestrate antiangiogenic resistance in glioblastoma through coordinated molecular networks, Cancer Letters (2015), doi: 10.1016/j.canlet.2015.09.004

Protein array

Differentially treated tumors were collected and isolated proteins were processed for mouse cytokine array (AAM-CYT-1000-8, Ray Biotech). Membranes were imaged using Las-3000 imaging machine (Fuji Film, Japan). All signals (expression intensity) emitted from the membrane were normalized to the positive control spots of corresponding membrane using Image J software. Later, expression intensities were imported as an excel file in Partek Genomic Suit 6.6 for heat map and box-plot analysis, and web based Ingenuity Pathway Analysis (IPA) interface for network analysis.

Statistical analysis

Quantitative data were expressed as mean ± SD and analyzed through Student t-test using GraphPad Prism. Differences were considered statistically significant at P value <0.05.

Results

Establishing chimeric mouse model

As reported before athymic nude mice (n = 3, each group) were transplanted with 5×10^6 BM cells from GFP+ mouse after whole body irradiation of sub-lethal dose (6Gy). Engraftment efficiency (GFP+) was determined at each week (days 7–56). Surprisingly, *i.v.* injection (n = 3) of 5×10^6 mononuclear cells achieved >70% engraftment by day 14 and >80% engraftment by day 56 (unpublished data). However, *i.p.* injection (n = 3) could achieve highest engraftment efficiency of 22.3% on day 56 (unpublished data). We used athymic nude mice in Balb/c background to establish chimera. Surprisingly, we did not observe any GVHD associated symptoms or mortality. Flow cytometry analysis using day 22 peripheral blood showed that 10–13% CD4 and 1–2% CD8 cells were transfused while establishing GFP+ chimeric mice (Supplementary Fig. S1). Further, we decided to use *i.v.* injection of 5×10^6 BM cells for 14 days to establish chimera for tumor studies.

Effect of GW2580 on tumor growth and GFP+ cell infiltration to the tumor

Chimeric animals were implanted with orthotopic glioma (U251) and treated with vehicle (n = 17), vatalanib (n = 10), GW2580 (n = 5) and GW2580+ vatalanib (n = 5) from days 8 to 21. All animals underwent MRI on day 22 following implantation of tumors. We observed significant reduction in tumor growth in GW2580 and GW2580+ vatalanib groups (Fig. 1A, upper left and right panels). *In vivo* optical images obtained on day 21 also showed increasing trend of cherry red+ tumor in vatalanib group and decreasing trend of cherry red+ tumor after treatments of GW2580 and GW2580+ vatalanib groups compared to vehicle (Fig. 1A, lower panel). Vatalanib treatment resulted in increasing trend of GFP+ cells accumulation in tumor. Decreasing trend of accumulation of GFP+ cells were observed in GW2580 and GW2580+ vatalanib groups compared to vehicle (Fig. 1B). Optical imaging data were validated by flow cytometry analysis, which proved increased infiltration of GFP+ cells in vatalanib group and decreased infiltration of GFP+ cells in tumors that were treated with GW2580 and GW2580+ vatalanib (Fig. 1C, upper and lower panels).

Effect of GW2580 on myeloid and endothelial cell signatures in tumor

Chimeric animals were implanted with orthotopic glioma (U251) and treated with vehicle, vatalanib, GW2580 and GW2580+vatalanib from days 8 to 21. Brain, spleen and BM (n = 3 each) were collected after MRI for flow cytometry analysis (Fig. 2A, upper and lower panels, spleen and BM data not shown). Infiltration of GFP+ cells was mostly seen at the periphery of the vatalanib treated tumor (Supplementary Fig. S2). Vatalanib treatment significantly increased CD68+ myeloid cells, and CD133+, CD34+ and CD202b+ or Tie2+ endothelial cell signatures. Significant decrease in myeloid (Gr1+ CD11b+ and F4/80+) and endothelial (CD202b+ and CD309+ or VEGFR2+) cell signatures were observed in GW2580 group compared to vehicle. However, CD133+ population was significantly increased in GW2580+ vatalanib group (upper and lower panels). Further, we observed that vatalanib induced endothelial marker expression was associated with the increased vasculature compared to vehicle group. This was characterized by increased CD31 expression on GFP+ cells. GW2580 treated tumors showed significantly decreased CD31 expression compared to vehicle and vatalanib treated groups (Supplementary Fig. S3). In immunofluorescence study, vatalanib treatment showed increased myeloid cell signatures (CD11b and F4/80) compared to vehicle (Fig. 2B). Decreased expression of myeloid cell signatures were observed following GW2580 and GW2580+ vatalanib treatments, compared to vehicle and vatalanib groups (Fig. 2B). Increasing trend of expression of immunosuppressive molecule, IDO, was seen with vatalanib, which was significantly decreased in GW2580 and GW2580+ vatalanib treated tumors (Fig. 2C).

Treatment induced molecular networks in GBM TME

U251 tumors were collected following vehicle, vatalanib, GW2580 and GW2580+ vatalanib treatment groups (n = 3 each). Tumor isolated proteins were processed for 96-plex protein array (Ray Biotech) followed by analysis of blots for expression intensities. Expression intensities were used to generate heatmap, which showed elevated expression of cytokines in following order of treatments; vatalanib > GW2580+ vatalanib > GW2580. Cytokines were mostly downregulated in GW2580 group and upregulated in vatalanib groups. Surprisingly, combination of vatalanib with GW2580 increased cytokine expression, which were decreased in GW2580 group (Fig. 3A and Supplementary Fig. S4). As represented by box-plot data, overall expression intensities were changed among groups. GW2580 group showed significantly decreased expression intensities of cytokines (Fig. 3B). By grouping cytokines based on their function, we found that GW2580 significantly decreased cytokines involved in inflammation (TCA3 or CCL11, TNFRI, CXCL9, GITR IL15, IL17, IL17RB, lungkine or CXCL15, MDC or CCL22, OPG, Resistin, Shh-N, TCK1 or CXCL7, TROY and TSLP), angiogenesis (bFGF, ICAM1, ITAC or CXCL11, VEGFR1,2,3 and VEGFD), proliferation and invasion (IL2, IL3, IL3RB, TIMP1,TIMP2, HGFR, IGFBP2, IGF1, IGF2, MMP2, MMP3 and Pro-MMP2). Notably, TCK1/CXCL7/macrophage derived growth factor/neutrophil activating peptide2 was observed as most significantly decreased cytokine in CSF1R inhibitor treatment compared to vehicle and other groups. In addition to TCK1, other decreased factors in GW2580 group, were elevated in vatalanib group (Fig. 3A and Supplementary Fig. S4). Since, we used mouse protein array; therefore, it is expected that tumor infiltrated BMDCs were sole source of all cytokines. Network analysis showed that ERK map kinase or P44/42 is a central and critical molecule for most of cytokines evaluated in protein array (Fig. 3C). Further, we tested if drug treated tumor tissues have dysregulated ERK map kinase pathway. Surprisingly, phosphorylated or active form (p-ERK) of ERK was increased after vatalanib treatment and decreased in GW2580 and GW2580+ vatalanib groups compared to vehicle (Fig. 3D).

Association of p-ERK expression with CXCL7 expression and proliferation

Immunofluorescence staining was performed to analyze the p-ERK expression on tumor tissues in all treated groups. We noticed expression of p-ERK in both tumor cells and tumor recruited GFP+ cells (more in tumor cells) in vehicle and vatalanib groups. Phospho-ERK expression in GFP+ cells is shown by white arrow heads. Please note significant decrease of GFP+ cells in both anti-CSF1R and

Please cite this article in press as: B.R. Achyut, Adarsh Shankar, A.S.M. Iskander, Roxan Ara, Kartik Angara, Peng Zeng, Robert A. Knight, Alfonso G. Scicli, Ali S. Arbab, Bone marrow derived myeloid cells orchestrate antiangiogenic resistance in glioblastoma through coordinated molecular networks, Cancer Letters (2015), doi: 10.1016/j.canlet.2015.09.004

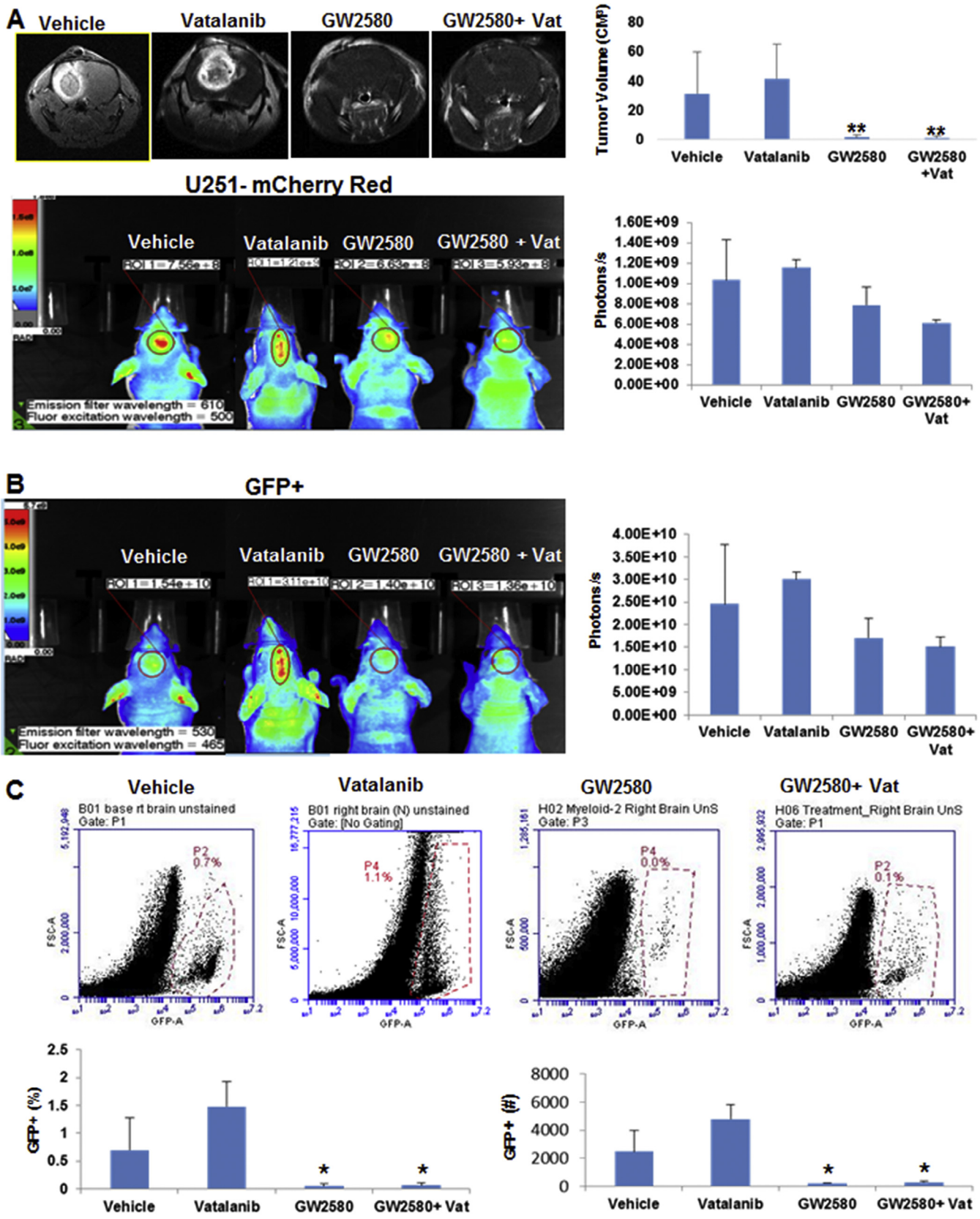

Fig. 1. Effect of vatalanib and CSF1R inhibitor on tumor growth and GFP+ cell infiltration to the tumor. (A) MRI images showing significant reduction in tumor growth in GW2580 and GW2580+ vatalanib groups (upper left and right panels) compared to vehicle. Vatalanib did not decrease tumor growth. *In vivo* optical images showing increasing trend of cherry red+ tumor in vatalanib group and decreasing trend of cherry red+ tumor after treatments of GW2580 and GW2580+ vatalanib groups compared to vehicle (Lower panels). (B) *In vivo* optical images showing increasing trend of GFP+ cells accumulation in tumor following vatalanib treatment and decreasing trend of accumulation of GFP+ cells in GW2580 and GW2580+ vatalanib groups compared to vehicle (C) Flow cytometry analysis showing increased infiltration of GFP+ cells in vatalanib group and decreased infiltration of GFP+ cells in tumors that were treated with GW2580 and GW2580+ vatalanib (upper and lower panels). Shown is one of the two experiments performed. Quantitative data are expressed in mean ± SD. *P < 0.05 and **P < 0.01.

Please cite this article in press as: B.R. Achyut, Adarsh Shankar, A.S.M. Iskander, Roxan Ara, Kartik Angara, Peng Zeng, Robert A. Knight, Alfonso G. Scicli, Ali S. Arbab, Bone marrow derived myeloid cells orchestrate antiangiogenic resistance in glioblastoma through coordinated molecular networks, Cancer Letters (2015), doi: 10.1016/j.canlet.2015.09.004

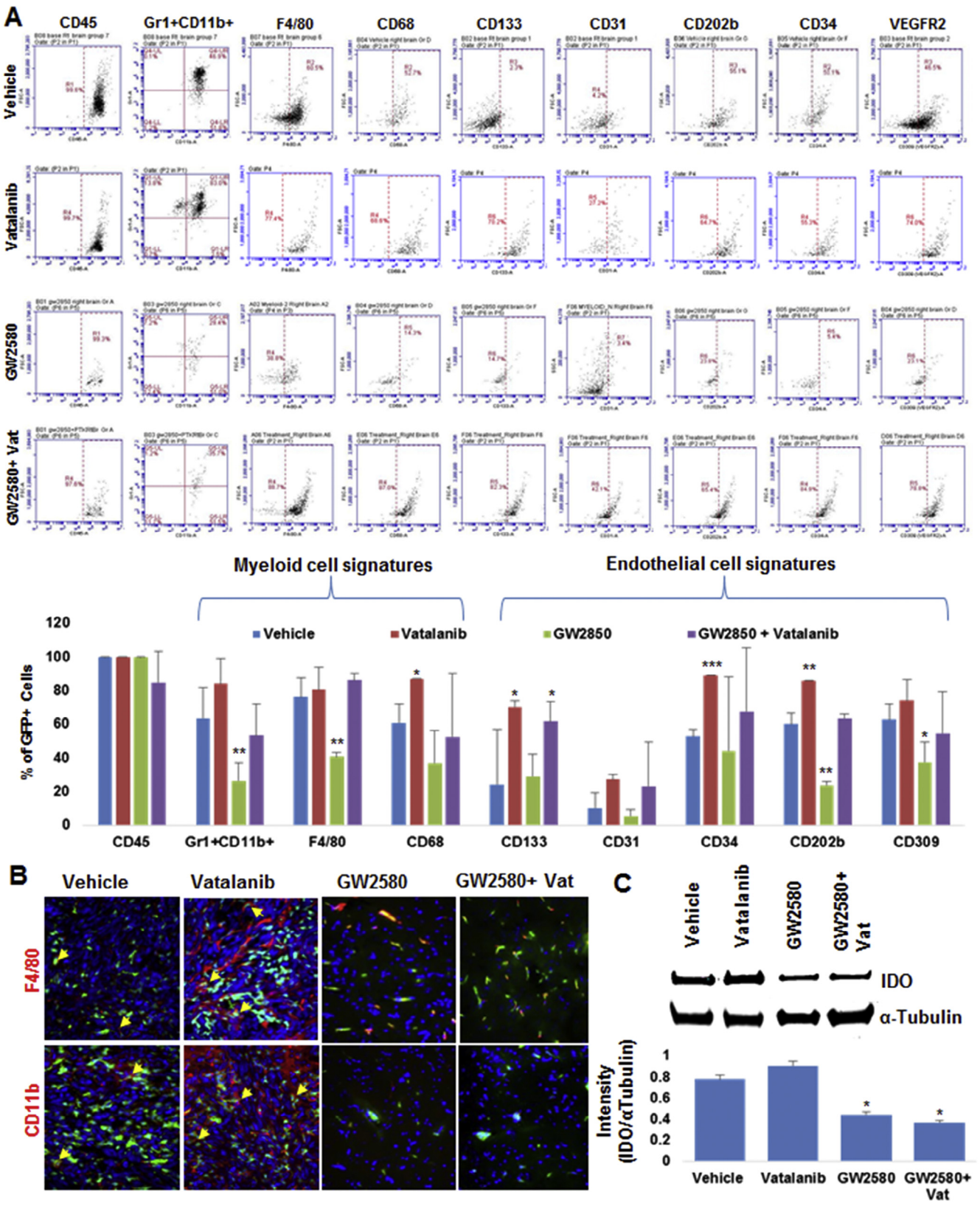

Fig. 2. Effect of vatalanib and CSF1R inhibitor on myeloid and endothelial cell signatures in GBM tumor. (A) Flow cytometry analysis showing significantly increased CD68+ myeloid cells, and CD133+, CD34+ and CD202b+ or Tie2+ endothelial cell signatures following vatalanib treatment. Significant decrease in myeloid (Gr1+ CD11b+ and F4/80+) and endothelial (CD202b+ or Tie2+ and CD309+ or VEGFR2+) cell signatures was seen following GW2580 treatment compared to vehicle. CD133+ population was significantly increased in GW2580+ vatalanib treated group (upper and lower panels). (B) Immunofluorescence study showing increased myeloid cell signatures (CD11b and F4/80) in vatalanib and decreased myeloid (CD11b and F4/80) markers following GW2580 and GW2580+ vatalanib treatments compared to vehicle (yellow arrows). (C) Western blot data showing increased IDO (immune suppressive) expression in vatalanib treated tumors, which were decreased in GW2580 and GW2580+ vatalanib groups (lower panels). Shown is one of the two experiments performed. Quantitative data are expressed in mean ± SD. *$P < 0.05$, **$P < 0.01$ and ***$P < 0.001$. (For interpretation of the references to color in this figure legend, the reader is referred to the web version of this article.)

Please cite this article in press as: B.R. Achyut, Adarsh Shankar, A.S.M. Iskander, Roxan Ara, Kartik Angara, Peng Zeng, Robert A. Knight, Alfonso G. Scicli, Ali S. Arbab, Bone marrow derived myeloid cells orchestrate antiangiogenic resistance in glioblastoma through coordinated molecular networks, Cancer Letters (2015), doi: 10.1016/j.canlet.2015.09.004

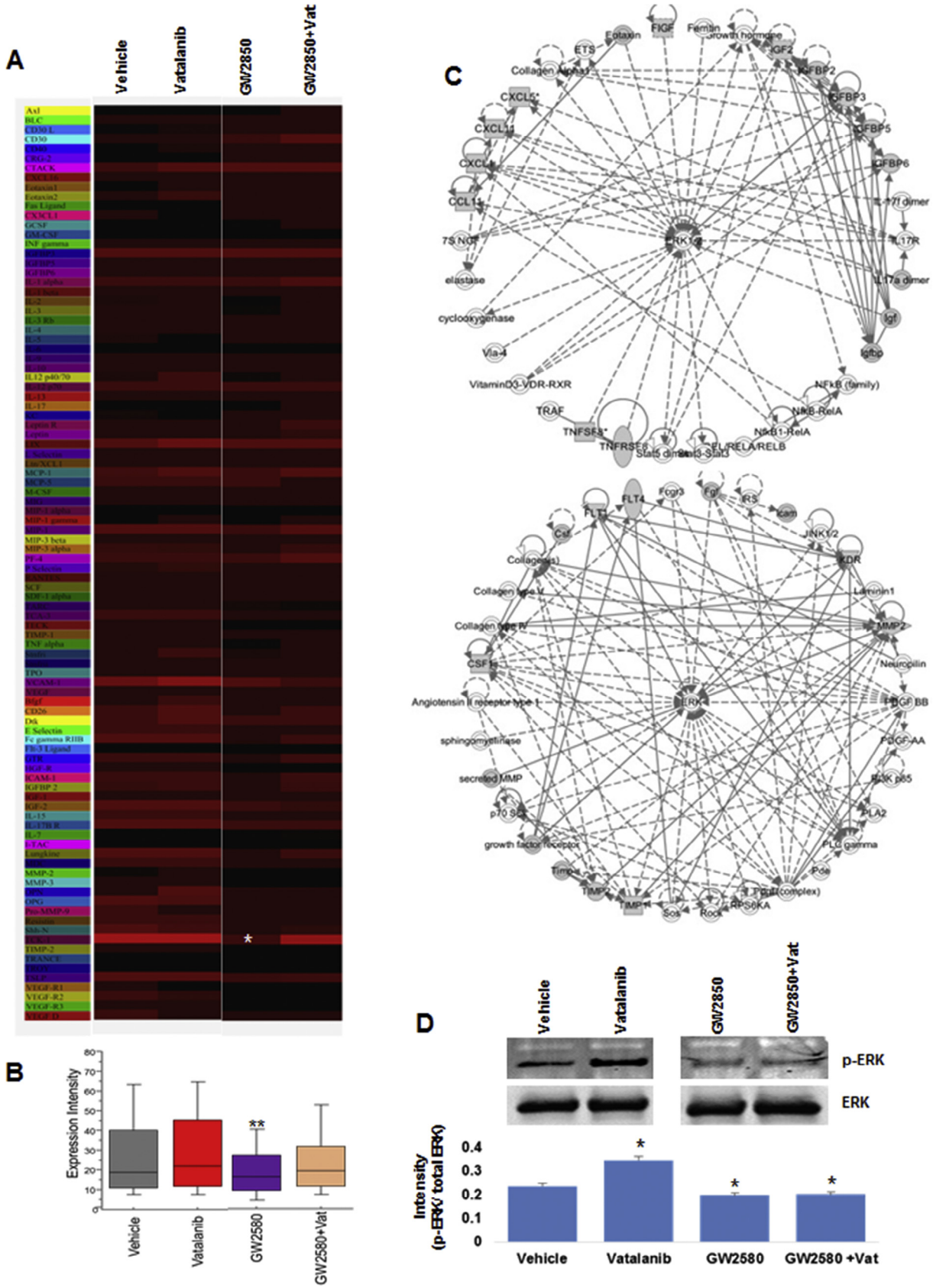

Fig. 3. Molecular networks in GBM TME. (A) Heatmap showing expression intensity of cytokine molecules following 96-plex protein array (Ray Biotech. These molecules were elevated in following order of treatment groups; vatalanib > GW2580+ vatalanib > GW2580. White star showing decreased expression of TCK1 or CCL7 following CSF1R blockade (B) Box-plot showing overall expression intensity changes among groups. GW2580 group showed significantly decreased expression intensity of molecules compared to other groups. (C) Network analysis showing ERK map kinase or P44/42 is a central molecule for cytokines (left panel). (D) Western blot using glioma tumor protein lysate showing increased expression of phosphorylated or active form (p-ERK) of ERK in vatalanib treatment and decreased in GW2580 and GW2580+ vatalanib groups (upper and lower panels). Shown is one of the two experiments performed. Quantitative data are expressed in mean ± SD. *P < 0.05 and **P < 0.01.

Please cite this article in press as: B.R. Achyut, Adarsh Shankar, A.S.M. Iskander, Roxan Ara, Kartik Angara, Peng Zeng, Robert A. Knight, Alfonso G. Scicli, Ali S. Arbab, Bone marrow derived myeloid cells orchestrate antiangiogenic resistance in glioblastoma through coordinated molecular networks, Cancer Letters (2015), doi: 10.1016/j.canlet.2015.09.004

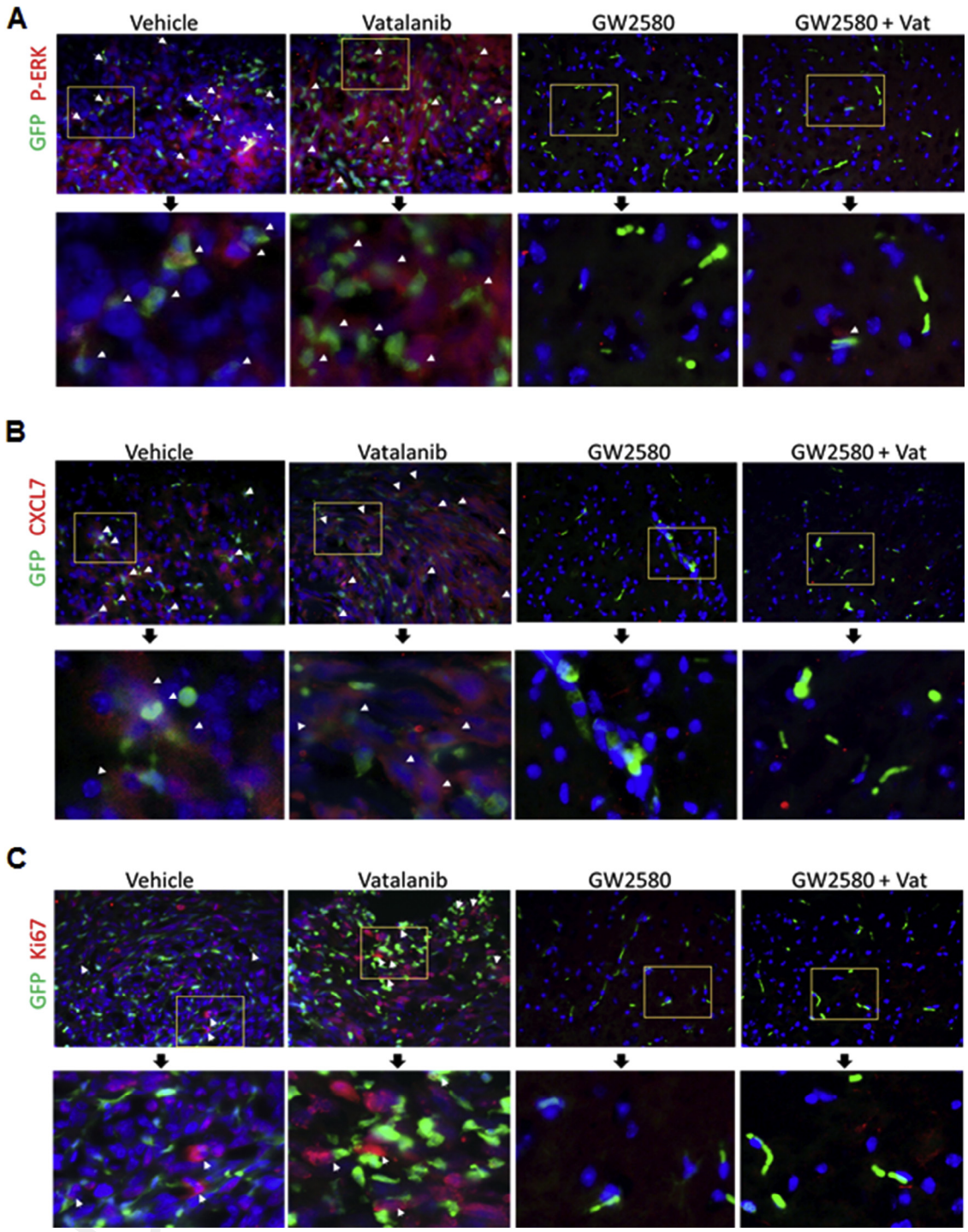

Fig. 4. Phospho-ERK expression is correlated with CXCL7 expression and proliferation. (A) Immunofluorescence analysis showing p-ERK expression in treated tumor tissues. Phospho-ERK expression was seen in both tumor cells and tumor recruited GFP+ cells in vehicle and vatalanib groups. Phospho-ERK expression in GFP+ cells is shown by white arrow heads. Anti-CSF1R and combination with vatalanib significant decreased of GFP+ cells in tumor and thus, decreased p-ERK expression in GFP+ cells. (B) Intracellular staining of CXCL7 on tumor tissues showing expression of CXCL7 in both tumor cells and tumor recruited GFP+ cells in vehicle and vatalanib groups. CXCL7 expression in GFP+ cells is shown by white arrow heads. GW2580 and its combination with vatalanib decreased GFP+ cells and thus, decreased CXCL7 expression in GFP+ cells. (C) Similarly, immunofluorescence staining of Ki67 on tumor tissues noticed expression of Ki67 in both tumor cells and tumor recruited GFP+ cells in vehicle and vatalanib groups. Ki67 expression in GFP+ cells is shown by white arrow heads. We found decreased GFP+ cells in both anti-CSF1R and combination with vatalanib and thus, decreased Ki67 expression in GFP+ cells.

combination with vatalanib and thus, decreased p-ERK expression in GFP+ cells (Fig. 4A). Intracellular staining of CXCL7 on tumor tissues was analyzed with all treated groups. We noticed expression of CXCL7 in both tumor cells and tumor recruited GFP+ cells (more in tumor cells) in vehicle and vatalanib groups. CXCL7 expression in GFP+ cells is shown by white arrow heads. Significant decrease of GFP+ cells was seen in both anti-CSF1R and combination with vatalanib and thus, decreased CXCL7 expression in GFP+ cells (Fig. 4B). Phospho-ERK has been known to involve in mitogen associated protein kinase (MAPK) pathway regulated proliferation

Please cite this article in press as: B.R. Achyut, Adarsh Shankar, A.S.M. Iskander, Roxan Ara, Kartik Angara, Peng Zeng, Robert A. Knight, Alfonso G. Scicli, Ali S. Arbab, Bone marrow derived myeloid cells orchestrate antiangiogenic resistance in glioblastoma through coordinated molecular networks, Cancer Letters (2015), doi: 10.1016/j.canlet.2015.09.004

hallmarks. We evaluated if p-ERK expression correlates with Ki67 proliferation data. Immunofluorescence staining of Ki67 on tumor tissues was analyzed in all treated groups. We noticed expression of Ki67 in both tumor cells and tumor recruited GFP+ cells (more in tumor cells) in vehicle and vatalanib groups. Ki67 expression in GFP+ cells is shown by white arrow heads. We found decreased GFP+ cells in both anti-CSF1R and combination with vatalanib and thus, decreased Ki67 expression in GFP+ cells (Fig. 4C).

Discussion

Since, GBM is hypervascular in nature, different drugs *e.g.* vatalanib, cediranib, sunitinib, etc. have been used against VEGF–VEGFR pathway to control abnormal angiogenesis in clinical trials [55–60]. Regrettably, benefits of AATs are at best transitory, and this period of clinical benefit is followed by restoration of tumor growth [61]. Evidence of relapse to progressive tumor growth reflects development of resistance to AATs [13,48]. In our previous study (under review in journal), we established a novel chimeric mouse model to study the contribution of BMDCs in tumor development and therapeutic resistance in GBM. We noticed increased infiltration of GFP+ BMDCs in TME and increased tumor growth as shown by MRI data following vatalanib, nintedanib and CXCR4 antagonist (AMD 3100). Treatments induced polarization of GFP+ BMDCs to the immunosuppressive myeloid cells. Therefore, in the present study, we intended to deplete the myeloid cells in the GBM TME. Similar to our report, other study reported that AATs increased infiltration in myeloid populations in the tumor bulk and in the infiltrative regions of the recurrent GBM (Supplementary Fig. S2) [23], which indicated requirement of myeloid cell inhibition in GBM.

So far, many myeloid inhibitors have been developed and have shown minimal to broad effect on myeloid cells [38,62–67]. GW2580, a selective small molecule kinase inhibitor of CSF1R, is an orally bioavailable competitive inhibitor of adenosine triphosphate binding [50]. GW2580 completely prevented CSF1R dependent growth of macrophages *in vitro* and *in vivo* at therapeutically relevant doses [50]. *In vitro* kinase assays with GW2580 demonstrated at least 100-fold selectivity for CSF1R compared with approximately 300 other structurally related and unrelated kinases [68]. Therefore, GW2580 have great therapeutic potential due to high selectivity and specificity for investigating the contributions of CSF1R signaling in the recruitment and polarization of different myeloid subsets *in vivo*.

In the present study, GW2580 was tested to inhibit CSF1R+ myeloid cells, which decreased tumor growth by decreasing GFP+ BMDCs acquiring myeloid cells(Gr1+ CD11b+ and F4/80+), angiogenic cells (CD202b+ and CD309+) and immune suppressive signature (IDO) [69]. Interestingly, expression of angiogenic markers on GFP+ cells was associated with the CD31+ vasculature in tumor tissues. In addition, mouse specific protein array data showed decreased expression of vasculature associated markers such as basic fibroblast growth factor (bFGF), vascular cell adhesion molecule 1(VCAM1), E-selectin or CD62 or endothelial-leukocyte adhesion molecule 1 (ELAM-1), intercellular Adhesion Molecule 1 (ICAM1) or CD54, vascular endothelial growth factor receptor 2 (VEGFR2) and VEGFR3 in GW2580 group. Altogether, data suggest that anti-CSF1R has profound effect on bone marrow cell contributed (GFP+) vasculature development (vasculogenesis). Previously, CSF1R inhibition using BLZ945 significantly increased survival and regressed established tumors. CSF1R blockade additionally slowed intracranial growth of patient-derived glioma xenografts. Surprisingly, TAMs were not depleted in treated mice. Instead, glioma-secreted factors, including GMCSF and IFN-γ, facilitated TAM survival in the context of CSF1R inhibition [70]. Our study suggested that GW2580 based CSF1R targeting has better myeloid inhibition compared to BLZ945 drug, which is further confirmed by study done by Xu et al. [43]. The authors showed that CSF1R signaling blockade stanched tumor-infiltrating myeloid cells and improved the efficacy of radiotherapy in prostate cancer [43].

Additionally, to evaluate any changes in cytotoxic T cell functions, we estimated cytokines involved in the T cell function using mouse specific cytokine array, for example, T cell activation (IL1), potent T cell growth factor (IL2), immuno-suppressive cytokine involved in T cell regulatory functions (IL10), helper T cell secreted cytokines that promote proliferation and differentiation of activated B cells (IL4 and IL5), cytokine involved in Th17 cell development (IL6) and Th17 secreted signature cytokine (IL17). We observed significant decreased IL2 cytokine in anti-CSF1R group and trend of increased IL6 and IL10 in anti-CSF1R+ vatalanib group compared to vehicle. This suggests that anti-CSF1R is better that combination treatment with vatalanib. Together, we believe that anti-CSF1R works profoundly through myeloid lineage with modest effect on T cell function.

We observed that combined treatments of GW2580 and vatalanib decreased tumor growth but promoted GFP+ cells to acquire CD133 phenotype in TME. CD133 phenotype has been shown to be associated with cancer stem cell and invasiveness properties [71]. This data clearly confirmed disadvantages associated with VEGFR2 targeting as shown by previous studies [46,56]. It is possible that decreased tumor growth by combined treatment is transient and tumor could regress due to increased CD133+ cells. However, survival studies are required to test this possibility. Our lab has previously observed similar data with sunitinib treatment against rat glioma, where sunitinib targeted both VEGFR2 and CSFR1. Sunitinib-treated animals showed significantly higher migration of the invasive cells [48]. Similar to our findings, other authors reported that angiogenesis inhibitor anti VEGFR2 antibody (DC101) induces morbidity, when combined with irradiation. In addition, combination therapy using GW2580 with an anti VEGFR2 antibody (DC101) synergistically suppressed tumor growth and severely impaired tumor angiogenesis along with reverting TAM mediated antiangiogenic compensatory mechanism involving MMP-9 [46]. We did not observe any decrease in myeloid and endothelial signature cells. There could be two reasons for this differential effect, firstly, our combination treatment started after the day 8 of the tumor implantation that allowed the tumor growth with microenvironment establishment. Our treatment schedule reflected clinical condition where glioma is diagnosed at later stage. On the other hand, a study done by Priceman et al. included same day treatment and tumor implantation with no sign of tumor establishment. Secondly, we cannot ignore the differential effects of antibody based and small molecule based protein kinase inhibitor targeting [72].

Several mechanisms have been known to regulate mobilization and recruitment immature myeloid cells into the TME, *e.g.* IL17 induced expression of GCSF through NF-κB and ERK signaling helped homing of myeloid cells to the tumor [21]. Bv8 modulated mobilization of MDSCs from BM to the tumor and promoted angiogenesis [29]. MDSC can be produced in BM in response to tumor derived factors *i.e.* GCSF, IL6, GMCSF, IL1β, PGE2 and TNFα, and were recruited to tumor site by CXCL12 and CXCL5 [40]. TGFβ signaling in BMDCs is important and recruits MDSCs via CCL2 in TME [73]. CEACAM1 is identified as negative regulator of myeloid cell expansion and recruitment by inhibiting GCSF-Bv8 axis [28]. Similarly, TIMP2 was shown to down regulate expression of immunosuppressive genes controlling MDSC growth such as IL10, IL13, IL11 and chemokine ligand (CCL5/RANTES), and increased IFN-γ and decreased CD40L [74]. In the present study, we performed 96-plex cytokine array to understand detailed molecular mechanisms and found aforementioned molecules and several other novel molecules involved in inflammation, angiogenesis, invasion and proliferation were downregulated after CSF1R inhibition. TCK1 or CXCL7, a potent chemoattractant and activator of neutrophils, was observed as most significantly decreased cytokine in CSF1R

Please cite this article in press as: B.R. Achyut, Adarsh Shankar, A.S.M. Iskander, Roxan Ara, Kartik Angara, Peng Zeng, Robert A. Knight, Alfonso G. Scicli, Ali S. Arbab, Bone marrow derived myeloid cells orchestrate antiangiogenic resistance in glioblastoma through coordinated molecular networks, Cancer Letters (2015), doi: 10.1016/j.canlet.2015.09.004

inhibition compared to vehicle and other groups (Fig. 3A, shown by star). Since, infiltration of GFP+ cells were significantly decreased after CSF1R blockade (Fig. 1C), we believe that decreased CXCL7 is associated with number of GFP+ cells in the TME. Notably, expression of CXCL7 reappeared in GW2580 and vatalanib combined treated tumors, which was associated with the increased GFP+ infiltration in tumor compared with GW2580 only group (Fig. 1C).

Biological significance of CXCL7 has been studied before, for example, CXCL7 co-localized with blood vessels, platelets and CD68+ macrophages. CXCL7 expression in synovial macrophages was associated with the inflamed rheumatoid arthritis [75]. In breast tumor, CXCL7, accompanied with IL6 has been shown to modulate human bone marrow mesenchymal cells traffic from the bone marrow to accelerate metastasis at distant sites by expanding the cancer stem cell population [76]. The authors showed that granulocyte recruitment in tumor was dependent on the secretion of CXCL5 and CXCL7 chemokines by platelets upon contact with tumor cells. Blockade of the CXCL5/7 receptor CXCR2, or transient depletion of either platelets or granulocytes prevents the formation of early metastatic niches and significantly reduces metastatic seeding and progression [77]. Proangiogenic and proinflammatory cytokine CXCL7 was an independent prognostic factor for overall survival of clear cell renal cell carcinoma (ccRCC). Inhibition of CXCL7 receptors CXCR1 and CXCR2 was sufficient to inhibit endothelial cell proliferation and ccRCC growth [78]. CXCR2 axis plays a key role in the recruitment of tumor-promoting neutrophils [79] and CXCR2-expressing MDSCs are essential to promote tumorigenesis [80]. In addition, we showed ERK MAPK pathway was involved in cytokine network regulation, which is associated with the CSF1R pathway in macrophages [81]. We believe that decreased p-ERK expression in GFP+ cells is associated with decreased cytokine expression (mouse specific) in GW2580 treated tumors. Moreover, Phospho-ERK has been known to involve in mitogen associated protein kinase (MAPK) pathway regulated proliferation hallmarks. We observed that p-ERK expression was correlated with Ki67 proliferation data. In addition, please note that mouse specific protein array data showed decreased expression of proliferation associated proteins such as IL2, IL3, IL3RB, TIMP1,TIMP2, HGFR, IGFBP2, IGF1, IGF2, MMP2, MMP3 and Pro-MMP2 in GW2580 group. Altogether, data suggest that anti-CSF1R has profound effect on bone marrow cell contributed (GFP+) proliferation events in GBM development.

In conclusion, the current study suggested the following: (1) myeloid cells are key players in GBM development and AAT resistance, (2) since CSF1R inhibition decreased cytokines (e.g.CXCL7) involved in inflammation, angiogenesis, invasion and proliferation; therefore, myeloid cells are major targets for therapeutic targeting in GBM. Clinical trials involving AATs were failed so far; therefore, our study for the first time provided a detailed investigation of altered myeloid cells and cytokine networks, sole cause of therapeutic resistance in GBM (Fig. 5). Nonetheless, survival studies are required to assess the beneficial effect of CSF1R blockade.

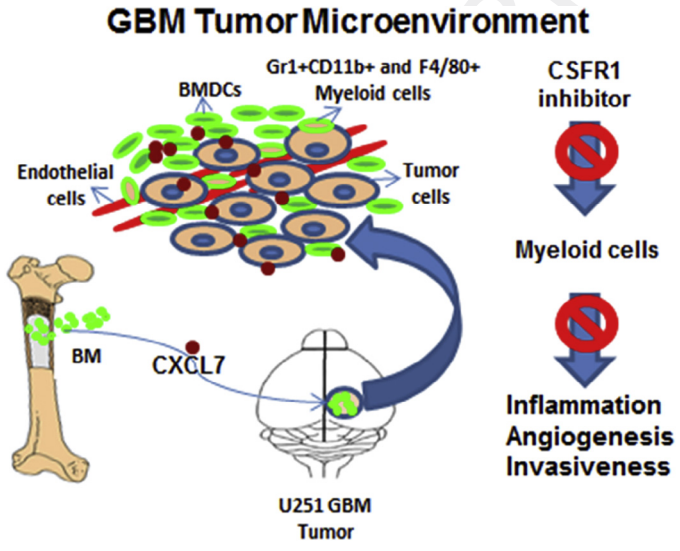

Fig. 5. Schematic representation of GBM TME. Orthotropic implantation of U251 cells in chimeric mouse initiated migration and homing of GFP+ BMDCs from BM to the tumor. GFP+ cells were found more concentrated at periphery or invasive front of tumor. These infiltrated GFP+ cells acquired myeloid phenotype under influence of tumor cell secreted factors and promoted tumor growth. Blocking CSF1R+ myeloid cells significantly reduced infiltration of GFP+ cells to the tumor and inhibited tumor growth by decreasing CXCL7 expression inflammation, angiogenesis, invasiveness and proliferation via inhibited myeloid cells.

Funding

Supported by the National Institutes of Health (NIH) grants R01CA160216 and R01CA172048.

Acknowledgement

The authors thank GRU Cancer Center Small Animal Imaging Core Facility for finishing project on timely manner. The authors thank Dr. Hasan Korkaya for providing 96-plex cytokine array (Ray Biotech).

Appendix: Supplementary material

Supplementary data to this article can be found online at doi:10.1016/j.canlet.2015.09.004.

References

[1] A. Olar, K.D. Aldape, Using the molecular classification of glioblastoma to inform personalized treatment, J. Pathol. 232 (2014) 165–177.
[2] R. Stupp, W.P. Mason, M.J. van den Bent, M. Weller, B. Fisher, M.J. Taphoorn, et al., Radiotherapy plus concomitant and adjuvant temozolomide for glioblastoma, N. Engl. J. Med. 352 (2005) 987–996.
[3] D.J. Brat, E.G. Van Meir, Vaso-occlusive and prothrombotic mechanisms associated with tumor hypoxia, necrosis, and accelerated growth in glioblastoma, Lab. Invest. 84 (2004) 397–405.
[4] R.K. Jain, Antiangiogenesis strategies revisited: from starving tumors to alleviating hypoxia, Cancer Cell 26 (2014) 605–622.
[5] Y. Zhao, A.A. Adjei, Targeting angiogenesis in cancer therapy: moving beyond vascular endothelial growth factor, Oncologist 20 (2015) 660–673.
[6] A.S. Arbab, Activation of alternative pathways of angiogenesis and involvement of stem cells following anti-angiogenesis treatment in glioma, Histol. Histopathol. 27 (2012) 549–557.
[7] S. Kumar, A.S. Arbab, Neovascularization in glioblastoma: current pitfall in anti-angiogenic therapy, Zhong Liu Za Zhi 1 (2013) 16–19.
[8] C.J. Scarlett, Contribution of bone marrow derived cells to the pancreatic tumor microenvironment, Frontiers in physiology 4 (2013) 56.
[9] M. Aghi, K.S. Cohen, R.J. Klein, D.T. Scadden, E.A. Chiocca, Tumor stromal-derived factor-1 recruits vascular progenitors to mitotic neovasculature, where microenvironment influences their differentiated phenotypes, Cancer Res. 66 (2006) 9054–9064.
[10] D.J. Ceradini, A.R. Kulkarni, M.J. Callaghan, O.M. Tepper, N. Bastidas, M.E. Kleinman, et al., Progenitor cell trafficking is regulated by hypoxic gradients through HIF-1 induction of SDF-1, Nat. Med. 10 (2004) 858–864.
[11] E. De Falco, D. Porcelli, A.R. Torella, S. Straino, M.G. Iachininoto, A. Orlandi, et al., SDF-1 involvement in endothelial phenotype and ischemia-induced recruitment of bone marrow progenitor cells, Blood 104 (2004) 3472–3482.
[12] R. Du, K.V. Lu, C. Petritsch, P. Liu, R. Ganss, E. Passegue, et al., HIF1alpha induces the recruitment of bone marrow-derived vascular modulatory cells to regulate tumor angiogenesis and invasion, Cancer Cell 13 (2008) 206–220.
[13] G. Bergers, D. Hanahan, Modes of resistance to anti-angiogenic therapy, Nat. Rev. Cancer 8 (2008) 592–603.
[14] Y. Huang, C. Hoffman, P. Rajappa, J.H. Kim, W. Hu, J. Huse, et al., Oligodendrocyte progenitor cells promote neovascularization in glioma by disrupting the blood-brain barrier, Cancer Res. 74 (2014) 1011–1021.
[15] G.O. Ahn, J.M. Brown, Matrix metalloproteinase-9 is required for tumor vasculogenesis but not for angiogenesis: role of bone marrow-derived myelomonocytic cells, Cancer Cell 13 (2008) 193–205.
[16] G.O. Ahn, J.M. Brown, Role of endothelial progenitors and other bone marrow-derived cells in the development of the tumor vasculature, Angiogenesis 12 (2009) 159–164.

Please cite this article in press as: B.R. Achyut, Adarsh Shankar, A.S.M. Iskander, Roxan Ara, Kartik Angara, Peng Zeng, Robert A. Knight, Alfonso G. Scicli, Ali S. Arbab, Bone marrow derived myeloid cells orchestrate antiangiogenic resistance in glioblastoma through coordinated molecular networks, Cancer Letters (2015), doi: 10.1016/j.canlet.2015.09.004

[17] E. Deak, S. Gottig, B. Ruster, V. Paunescu, E. Seifried, J. Gille, et al., Bone marrow derived cells in the tumour microenvironment contain cells with primitive haematopoietic phenotype, J. Cell. Mol. Med. 14 (2010) 1946–1952.
[18] V.R. Shinde Patil, E.B. Friedrich, A.E. Wolley, R.E. Gerszten, J.R. Allport, R. Weissleder, Bone marrow-derived lin(-)c-kit(+)Sca-1+ stem cells do not contribute to vasculogenesis in Lewis lung carcinoma, Neoplasia 7 (2005) 234–240.
[19] M. Seandel, J. Butler, D. Lyden, S. Rafii, A catalytic role for proangiogenic marrow-derived cells in tumor neovascularization, Cancer Cell 13 (2008) 181–183.
[20] B.R. Achyut, Impact of microenvironment in therapy-induced neovascularization of glioblastoma, Biochem. Physiol. 2 (2013) e121.
[21] A.S. Chung, X. Wu, G. Zhuang, H. Ngu, I. Kasman, J. Zhang, et al., An interleukin-17-mediated paracrine network promotes tumor resistance to anti-angiogenic therapy, Nat. Med. 19 (2013) 1114–1123.
[22] E. Dondossola, R. Rangel, L. Guzman-Rojas, E.M. Barbu, H. Hosoya, L.S. St John, et al., CD13-positive bone marrow-derived myeloid cells promote angiogenesis, tumor growth, and metastasis, Proc. Natl. Acad. Sci. U.S.A. 110 (2013) 20717–20722.
[23] C. Lu-Emerson, M. Snuderl, N.D. Kirkpatrick, J. Goveia, C. Davidson, Y. Huang, et al., Increase in tumor-associated macrophages after antiangiogenic therapy is associated with poor survival among patients with recurrent glioblastoma, Neuro-Oncol. 15 (2013) 1079–1087.
[24] V.T. Phan, X. Wu, J.H. Cheng, R.X. Sheng, A.S. Chung, G. Zhuang, et al., Oncogenic RAS pathway activation promotes resistance to anti-VEGF therapy through G-CSF-induced neutrophil recruitment, Proc. Natl. Acad. Sci. U.S.A. 110 (2013) 6079–6084.
[25] S. Seton-Rogers, Tumour microenvironment: means of resistance, Nat. Rev. Cancer 13 (2013) 607.
[26] F. Shojaei, X. Wu, X. Qu, M. Kowanetz, L. Yu, M. Tan, et al., G-CSF-initiated myeloid cell mobilization and angiogenesis mediate tumor refractoriness to anti-VEGF therapy in mouse models, Proc. Natl. Acad. Sci. U.S.A. 106 (2009) 6742–6747.
[27] B.R. Achyut, A.S. Arbab, Myeloid derived suppressor cells: fuel the fire, Biochem. Physiol. 3 (2014) e123.
[28] R. Lu, M. Kujawski, H. Pan, J.E. Shively, Tumor angiogenesis mediated by myeloid cells is negatively regulated by CEACAM1, Cancer Res. 72 (2012) 2239–2250.
[29] F. Shojaei, X. Wu, C. Zhong, L. Yu, X.H. Liang, J. Yao, et al., Bv8 regulates myeloid-cell-dependent tumour angiogenesis, Nature 450 (2007) 825–831.
[30] F. Shojaei, C. Zhong, X. Wu, L. Yu, N. Ferrara, Role of myeloid cells in tumor angiogenesis and growth, Trends Cell Biol. 18 (2008) 372–378.
[31] L. Yang, L.M. DeBusk, K. Fukuda, B. Fingleton, B. Green-Jarvis, Y. Shyr, et al., Expansion of myeloid immune suppressor Gr+CD11b+ cells in tumor-bearing host directly promotes tumor angiogenesis, Cancer Cell 6 (2004) 409–421.
[32] E. Gomez Perdiguero, K. Klapproth, C. Schulz, K. Busch, E. Azzoni, L. Crozet, et al., Tissue-resident macrophages originate from yolk-sac-derived erythro-myeloid progenitors, Nature 518 (2015) 547–551.
[33] S.C. Wang, J.H. Hong, C. Hsueh, C.S. Chiang, Tumor-secreted SDF-1 promotes glioma invasiveness and TAM tropism toward hypoxia in a murine astrocytoma model, Lab. Invest. 92 (2012) 151–162.
[34] Y. Piao, J. Liang, L. Holmes, A.J. Zurita, V. Henry, J.V. Heymach, et al., Glioblastoma resistance to anti-VEGF therapy is associated with myeloid cell infiltration, stem cell accumulation, and a mesenchymal phenotype, Neuro-Oncol. 14 (2012) 1379–1392.
[35] M.R. Galdiero, E. Bonavita, I. Barajon, C. Garlanda, A. Mantovani, S. Jaillon, Tumor associated macrophages and neutrophils in cancer, Immunobiology 218 (2013) 1402–1410.
[36] S.F. Hussain, D. Yang, D. Suki, K. Aldape, E. Grimm, A.B. Heimberger, The role of human glioma-infiltrating microglia/macrophages in mediating antitumor immune responses, Neuro-Oncol. 8 (2006) 261–279.
[37] A. Sica, T. Schioppa, A. Mantovani, P. Allavena, Tumour-associated macrophages are a distinct M2 polarised population promoting tumour progression: potential targets of anti-cancer therapy, Eur. J. Cancer 42 (2006) 717–727.
[38] R. Wesolowski, J. Markowitz, W.E. Carson 3rd, Myeloid derived suppressor cells – a new therapeutic target in the treatment of cancer, J. Immunother. Cancer 1 (2013) 10.
[39] E.Y. Lin, A.V. Nguyen, R.G. Russell, J.W. Pollard, Colony-stimulating factor 1 promotes progression of mammary tumors to malignancy, J. Exp. Med. 193 (2001) 727–740.
[40] Y. Sawanobori, S. Ueha, M. Kurachi, T. Shimaoka, J.E. Talmadge, J. Abe, et al., Chemokine-mediated rapid turnover of myeloid-derived suppressor cells in tumor-bearing mice, Blood 111 (2008) 5457–5466.
[41] K.P. MacDonald, V. Rowe, H.M. Bofinger, R. Thomas, T. Sasmono, D.A. Hume, et al., The colony-stimulating factor 1 receptor is expressed on dendritic cells during differentiation and regulates their expansion, J. Immunol. 175 (2005) 1399–1405.
[42] K. Movahedi, M. Guilliams, J. Van den Bossche, R. Van den Bergh, C. Gysemans, A. Beschin, et al., Identification of discrete tumor-induced myeloid-derived suppressor cell subpopulations with distinct T cell-suppressive activity, Blood 111 (2008) 4233–4244.
[43] J. Xu, J. Escamilla, S. Mok, J. David, S. Priceman, B. West, et al., CSF1R signaling blockade stanches tumor-infiltrating myeloid cells and improves the efficacy of radiotherapy in prostate cancer, Cancer Res. 73 (2013) 2782–2794.
[44] J.A. Hamilton, Colony-stimulating factors in inflammation and autoimmunity, Nat. Rev. Immunol. 8 (2008) 533–544.
[45] D.A. Hume, K.P. MacDonald, Therapeutic applications of macrophage colony-stimulating factor-1 (CSF-1) and antagonists of CSF-1 receptor (CSF-1R) signaling, Blood 119 (2012) 1810–1820.
[46] S.J. Priceman, J.L. Sung, Z. Shaposhnik, J.B. Burton, A.X. Torres-Collado, D.L. Moughon, et al., Targeting distinct tumor-infiltrating myeloid cells by inhibiting CSF-1 receptor: combating tumor evasion of antiangiogenic therapy, Blood 115 (2010) 1461–1471.
[47] Y. Zhu, B.L. Knolhoff, M.A. Meyer, T.M. Nywening, B.L. West, J. Luo, et al., CSF1/CSF1R blockade reprograms tumor-infiltrating macrophages and improves response to T-cell checkpoint immunotherapy in pancreatic cancer models, Cancer Res. 74 (2014) 5057–5069.
[48] M.M. Ali, S. Kumar, A. Shankar, N.R. Varma, A.S. Iskander, B. Janic, et al., Effects of tyrosine kinase inhibitors and CXCR4 antagonist on tumor growth and angiogenesis in rat glioma model: MRI and protein analysis study, Transl. Oncol. 6 (2013) 660–669.
[49] D.A. Yuen, B.E. Stead, Y. Zhang, K.E. White, M.G. Kabir, K. Thai, et al., eNOS deficiency predisposes podocytes to injury in diabetes, J. Am. Soc. Nephrol. 23 (2012) 1810–1823.
[50] J.G. Conway, B. McDonald, J. Parham, B. Keith, D.W. Rusnak, E. Shaw, et al., Inhibition of colony-stimulating-factor-1 signaling in vivo with the orally bioavailable cFMS kinase inhibitor GW2580, Proc. Natl. Acad. Sci. U.S.A. 102 (2005) 16078–16083.
[51] G. Ding, Q. Jiang, L. Zhang, Z.G. Zhang, L. Li, R.A. Knight, et al., Analysis of combined treatment of embolic stroke in rat with r-tPA and a GPIIb/IIIa inhibitor, J. Cereb. Blood Flow Metab. 25 (2005) 87–97.
[52] J.R. Ewing, R.A. Knight, T.N. Nagaraja, J.S. Yee, V. Nagesh, P.A. Whitton, et al., Patlak plots of Gd-DTPA MRI data yield blood-brain transfer constants concordant with those of 14C-sucrose in areas of blood-brain opening, Magn. Reson. Med. 50 (2003) 283–292.
[53] T.N. Nagaraja, K. Karki, J.R. Ewing, R.L. Croxen, R.A. Knight, Identification of variations in blood-brain barrier opening after cerebral ischemia by dual contrast-enhanced magnetic resonance imaging and t1sat measurements, Stroke 39 (2008) 427–432.
[54] T.N. Nagaraja, K. Karki, J.R. Ewing, G.W. Divine, J.D. Fenstermacher, C.S. Patlak, et al., The MRI-measured arterial input function resulting from a bolus injection of Gd-DTPA in a rat model of stroke slightly underestimates that of Gd-[14C]DTPA and marginally overestimates the blood-to-brain influx rate constant determined by Patlak plots, Magn. Reson. Med. 63 (2010) 1502–1509.
[55] A. Bruno, A. Pagani, E. Magnani, T. Rossi, D.M. Noonan, A.R. Cantelmo, et al., Inflammatory angiogenesis and the tumor microenvironment as targets for cancer therapy and prevention, Cancer Treat. Res. 159 (2014) 401–426.
[56] J. Dietrich, A.D. Norden, P.Y. Wen, Emerging antiangiogenic treatments for gliomas – efficacy and safety issues, Curr. Opin. Neurol. 21 (2008) 736–744.
[57] K. Mittal, J. Ebos, B. Rini, Angiogenesis and the tumor microenvironment: vascular endothelial growth factor and beyond, Semin. Oncol. 41 (2014) 235–251.
[58] R. Rahman, S. Smith, C. Rahman, R. Grundy, Antiangiogenic therapy and mechanisms of tumor resistance in malignant glioma, J. Oncol. 2010 (2010) 251231.
[59] P. Saharinen, L. Eklund, K. Pulkki, P. Bono, K. Alitalo, VEGF and angiopoietin signaling in tumor angiogenesis and metastasis, Trends Mol. Med. 17 (2011) 347–362.
[60] J. Samples, M. Willis, N. Klauber-DeMore, Targeting angiogenesis and the tumor microenvironment, Surg. Oncol. Clin. N. Am. 22 (2013) 629.
[61] K.D. Miller, C.J. Sweeney, G.W. Sledge Jr., Can tumor angiogenesis be inhibited without resistance?, EXS (2005) 95–112.
[62] D. Alizadeh, N. Larmonier, Chemotherapeutic targeting of cancer-induced immunosuppressive cells, Cancer Res. 74 (2014) 2663–2668.
[63] M. Bruchard, F. Ghiringhelli, Impact of chemotherapies on immunosuppression and discovery of new therapeutic targets, Bull. Cancer 101 (2014) 605–607.
[64] S.L. Highfill, Y. Cui, A.J. Giles, J.P. Smith, H. Zhang, E. Morse, et al., Disruption of CXCR2-mediated MDSC tumor trafficking enhances anti-PD1 efficacy, Sci. Transl. Med. 6 (2014) 237ra267.
[65] Y. Mao, D. Sarhan, A. Steven, B. Seliger, R. Kiessling, A. Lundqvist, Inhibition of tumor-derived prostaglandin-E2 blocks the induction of myeloid-derived suppressor cells and recovers natural killer cell activity, Clin. Cancer Res. 20 (15) (2014) 4096–4106.
[66] B.L. Mundy-Bosse, G.B. Lesinski, A.C. Jaime-Ramirez, K. Benninger, M. Khan, P. Kuppusamy, et al., Myeloid-derived suppressor cell inhibition of the IFN response in tumor-bearing mice, Cancer Res. 71 (2011) 5101–5110.
[67] H. Qin, B. Lerman, I. Sakamaki, G. Wei, S.C. Cha, S.S. Rao, et al., Generation of a new therapeutic peptide that depletes myeloid-derived suppressor cells in tumor-bearing mice, Nat. Med. 20 (2014) 676–681.
[68] M.W. Karaman, S. Herrgard, D.K. Treiber, P. Gallant, C.E. Atteridge, B.T. Campbell, et al., A quantitative analysis of kinase inhibitor selectivity, Nat. Biotechnol. 26 (2008) 127–132.
[69] J. Yu, Y. Wang, F. Yan, P. Zhang, H. Li, H. Zhao, et al., Noncanonical NF-kappaB activation mediates STAT3-stimulated IDO upregulation in myeloid-derived suppressor cells in breast cancer, J. Immunol. 193 (2014) 2574–2586.
[70] S.M. Pyonteck, L. Akkari, A.J. Schuhmacher, R.L. Bowman, L. Sevenich, D.F. Quail, et al., CSF-1R inhibition alters macrophage polarization and blocks glioma progression, Nat. Med. 19 (2013) 1264–1272.
[71] B. Annabi, S. Rojas-Sutterlin, C. Laflamme, M.P. Lachambre, Y. Rolland, H. Sartelet, et al., Tumor environment dictates medulloblastoma cancer stem cell expression and invasive phenotype, Mol. Cancer Res. 6 (2008) 907–916.

Please cite this article in press as: B.R. Achyut, Adarsh Shankar, A.S.M. Iskander, Roxan Ara, Kartik Angara, Peng Zeng, Robert A. Knight, Alfonso G. Scicli, Ali S. Arbab, Bone marrow derived myeloid cells orchestrate antiangiogenic resistance in glioblastoma through coordinated molecular networks, Cancer Letters (2015), doi: 10.1016/j.canlet.2015.09.004

[72] K. Imai, A. Takaoka, Comparing antibody and small-molecule therapies for cancer, Nat. Rev. Cancer 6 (2006) 714–727.
[73] Q. Fan, D. Gu, H. Liu, L. Yang, X. Zhang, M.C. Yoder, et al., Defective TGF-beta signaling in bone marrow-derived cells prevents hedgehog-induced skin tumors, Cancer Res. 74 (2014) 471–483.
[74] L. Guedez, S. Jensen-Taubman, D. Bourboulia, C.J. Kwityn, B. Wei, J. Caterina, et al., TIMP-2 targets tumor-associated myeloid suppressor cells with effects in cancer immune dysfunction and angiogenesis, J. Immunother. 35 (2012) 502–512.
[75] L. Yeo, N. Adlard, M. Biehl, M. Juarez, T. Smallie, M. Snow, et al., Expression of chemokines CXCL4 and CXCL7 by synovial macrophages defines an early stage of rheumatoid arthritis, Ann. Rheum. Dis. (2015) doi:10.1136/annrheumdis-2014-206921.
[76] S. Liu, C. Ginestier, S.J. Ou, S.G. Clouthier, S.H. Patel, F. Monville, et al., Breast cancer stem cells are regulated by mesenchymal stem cells through cytokine networks, Cancer Res. 71 (2011) 614–624.
[77] M. Labelle, S. Begum, R.O. Hynes, Platelets guide the formation of early metastatic niches, Proc. Natl. Acad. Sci. U.S.A. 111 (2014) E3053–E3061.
[78] R. Grepin, M. Guyot, S. Giuliano, M. Boncompagni, D. Ambrosetti, E. Chamorey, et al., The CXCL7/CXCR1/2 axis is a key driver in the growth of clear cell renal cell carcinoma, Cancer Res. 74 (2014) 873–883.
[79] L. Raccosta, R. Fontana, D. Maggioni, C. Lanterna, E.J. Villablanca, A. Paniccia, et al., The oxysterol-CXCR2 axis plays a key role in the recruitment of tumor-promoting neutrophils, J. Exp. Med. 210 (2013) 1711–1728.
[80] H. Katoh, D. Wang, T. Daikoku, H. Sun, S.K. Dey, R.N. Dubois, CXCR2-expressing myeloid-derived suppressor cells are essential to promote colitis-associated tumorigenesis, Cancer Cell 24 (2013) 631–644.
[81] J. Huynh, M.Q. Kwa, A.D. Cook, J.A. Hamilton, G.M. Scholz, CSF-1 receptor signalling from endosomes mediates the sustained activation of Erk1/2 and Akt in macrophages, Cell. Signal. 24 (2012) 1753–1761.

Please cite this article in press as: B.R. Achyut, Adarsh Shankar, A.S.M. Iskander, Roxan Ara, Kartik Angara, Peng Zeng, Robert A. Knight, Alfonso G. Scicli, Ali S. Arbab, Bone marrow derived myeloid cells orchestrate antiangiogenic resistance in glioblastoma through coordinated molecular networks, Cancer Letters (2015), doi: 10.1016/j.canlet.2015.09.004